

Molecular docking guided structure based design of symmetrical N,N'-disubstituted urea/thiourea as HIV-1 gp120–CD4 binding inhibitors



Sree Kanth Sivan, Radhika Vangala, Vijjulatha Manga*

Molecular Modeling and Medicinal Chemistry Group, Department of Chemistry, Nizam College, Hyderabad 500001, India

ARTICLE INFO

Article history:

Received 14 February 2013

Revised 16 May 2013

Accepted 17 May 2013

Available online 1 June 2013

Keywords:

HIV-1 gp120

Symmetrical N,N'-disubstituted urea

Symmetrical N,N'-disubstituted thiourea

Molecular docking

Induced fit docking (IFD)

Enzyme-linked immunosorbent assay

(ELISA)

ABSTRACT

Induced fit molecular docking studies were performed on BMS-806 derivatives reported as small molecule inhibitors of HIV-1 gp120–CD4 binding. Comprehensive study of protein–ligand interactions guided in identification and design of novel symmetrical N,N'-disubstituted urea and thiourea as HIV-1 gp120–CD4 binding inhibitors. These molecules were synthesized in aqueous medium using microwave irradiation. Synthesized molecules were screened for their inhibitory ability by HIV-1 gp120–CD4 capture enzyme-linked immunosorbent assay (ELISA). Designed compounds were found to inhibit HIV-1 gp120–CD4 binding in micromolar (0.013–0.247 μM) concentrations.

© 2013 Elsevier Ltd. All rights reserved.

1. Introduction

HIV-1 cell entry is mediated by sequential interactions of envelope protein gp120 with the receptor CD4 and a co-receptor, usually CCR5 or CXCR4, depending on the individual virion. Entry of primate immunodeficiency viruses into the host cell involves binding of HIV-1 gp120–CD4 glycoprotein, which serves as the primary receptor.¹ This binding creates the necessary exposure of an interacting surface for the CCR5 or CXCR4 host-cell chemokine receptor. This chain of events triggers the release of HIV-1 gp41 which, ultimately, undergoes a large conformational change responsible for the viral and cellular membranes apposition, thereby allowing entry of viral genetic material into the cytosol.^{2,3} This series of HIV-1 Env–receptor interactions are the major focus of research aimed at developing broadly neutralizing antibodies to interrupt the entry process. Extensive Env glycosylation and conformational masking of the functional spike (i.e., epitope inaccessibility) make this glycoprotein a difficult target for broadly neutralizing antibodies.^{4–6} Receptor-binding structures of HIV-1 gp120 are conserved among diverse viral isolates and represent functionally constrained regions that might serve as targets of broadly neutralizing antibodies. However, evidence from structural studies suggest that,

within functional spike, the CD4-binding site (CD4bs) is a recessed pocket and the co-receptor-binding site (or CD4-induced region) is either not formed or not exposed until HIV-1 gp120 engages CD4 on target cells.⁷ During this highly coordinated process, conserved hidden epitopes in Env are exposed to the surface. Targeting these highly conserved transiently exposed epitopes as well as conformational epitopes generated by the CD4–HIV-1 gp120–CCR5/CXCR4 complex by antivirals, may limit significantly viral escape and broaden the antiviral activity of inhibitory molecules to effectively neutralize a wide range of HIV-1 clades.

Most of the potent HIV-1 gp120–CD4 inhibitors identified till date are proteins or peptides.⁸ However recent publications and patent disclosures indicate that there has been an increased effort to identify small-molecule HIV-1 gp120 inhibitors that can block HIV-1 gp120–CD4 interactions.⁹ BMS-378806 (BMS-806) and BMS-4880434 discovered through a cell-based screening assay (HIV-1 envelope-mediated fusion assay using two populations of HeLa cells),¹⁰ are potent small-molecule inhibitors that are reported to prevent the binding of HIV-1 gp120–CD4 receptors in nanomolar range.^{10–12} NBD-556 and NBD-557 identified by a HIV syncytium formation assay on a drug-like small-molecule chemical library of 33,000 compounds have been reported to exhibit single digit micromolar potency against selected HIV-1 laboratory strains with minimal cytotoxicity.¹³

Tamamur and co-workers^{14–16} have designed and synthesised small molecule CD4 mimics (NBD-556 derivatives) that inhibit

* Corresponding author. Tel.: +91 9866845408.

E-mail addresses: sivan.sreekanth@gmail.com (S.K. Sivan), vangalaradhika@yahoo.com (R. Vangala), vijjulathamanga@gmail.com (V. Manga).

gp120–CD4 interactions. These molecules possess substituted phenyl groups attached to oxalamide group at one end and piperidinyll group at the other end. Molecular docking studies illustrated a hydrophobic interaction between phenyl group and hydrophobic residues in the binding site of gp120. The piperidinyll moiety has an electrostatic interaction with Asp368 and a hydrophobic interaction with Val430. Similar interactions were reported by Bewley et al.¹⁸ for batzelladine analogues, and these were further optimized by Kazuo Nagasawa et al.¹⁷

In present work novel symmetrical substituted urea and thio-urea having benzimidazole moieties were designed based on molecular docking studies, these were synthesized and analyzed for their inhibitory activity against gp120–CD4 interaction.

2. Results and discussion

HIV-1 gp120 core is composed of inner and outer domains, which reflects the likely orientation of HIV-1 gp120 in the assembled trimer, and a bridging sheet. Components of both domains and the bridging sheet contribute to CD4 binding. CD4 binds in a

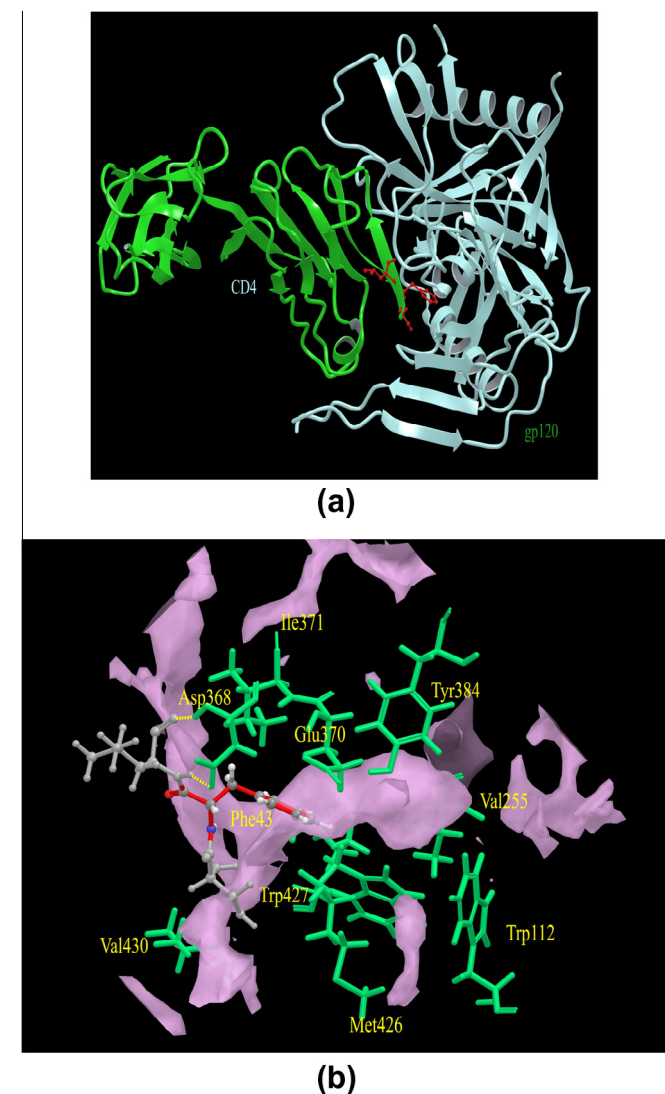


Figure 1. (a) Crystal structure of HIV-1 gp120 with soluble CD4 retrieved from the PDB (id: 1RZJ), showing Phe43 of CD4 binding with HIV-1 gp120. (b) Focused view of Phe43 binding cavity of HIV-1 gp120, the hydrophobic region is represent in pink, Phe43 residue of CD4 is shown in red, it shows hydrogen bond interactions with Asp368 of HIV-1 gp120.

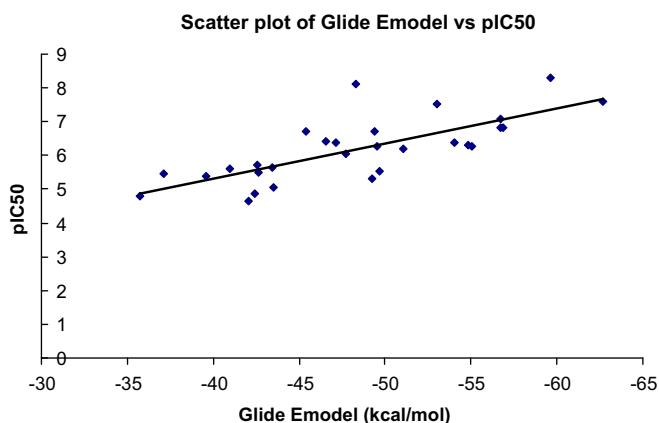


Figure 2. Scatter plot of Glide Emodel (kcal/mol) versus experimental pIC₅₀.

recessed pocket on HIV-1 gp120 to a surface that is larger than that occluded by a typical antibody–protein interaction. The interface displays several unusual features, including a shallow, water-filled cavity that is thought to function in immune evasion. A second interfacial cavity penetrates into the hydrophobic interior of HIV-1 gp120; it is bounded by conserved interior HIV-1 gp120 residues derived from all three domains and by Phe43 of CD4 (Fig. 1). Mutagenesis, conservation and structural analysis all indicate that this “Phe43 cavity” and its surrounding structures are critically important for CD4 binding. Phe43 cavity thus constitutes a conserved, spatially localized feature in a large, otherwise relatively variable HIV-1 gp120–CD4 interface. Consequently, the CD4–gp120 cavity has been suggested to be a potential target for drug design.^{19,20}

On the basis of the consideration that Phe43 cavity is highly conserved and has been hypothesized to be a site less prone to

Table 1
Experimental pIC₅₀, Glide Score, Emodel and predicted activity of BMS derivatives

Compound	pIC ₅₀	Glide Score (XP) (kcal/mol)	Emodel (kcal/ mol)	Predicted activity
1	8.097	-7.166	-48.269	6.184
2	6.284	-7.541	-49.560	6.321
3	7.523	-7.403	-52.988	6.683
4	7.588	-8.305	-62.656	7.706
5	8.301	-7.552	-59.619	7.385
6	6.066	-7.537	-47.683	6.122
7	6.377	-6.099	-54.007	6.791
8	6.284	-5.560	-55.084	6.905
9	5.721	-6.308	-42.554	5.579
10	5.638	-6.484	-43.450	5.674
11	5.620	-7.233	-40.937	5.408
12	5.523	-8.008	-49.651	6.330
13	5.481	-6.758	-42.636	5.588
14	5.041	-7.212	-43.510	5.681
15	4.657	-7.360	-42.076	5.529
16	4.796	-5.797	-35.740	4.859
17	4.886	-6.924	-42.413	5.565
18	6.367	-7.630	-47.147	6.065
19	6.699	-6.769	-45.392	5.879
20	6.432	-6.308	-46.540	6.001
21	5.328	-6.768	-49.274	6.290
22	5.372	-7.132	-39.607	5.268
23	5.444	-6.784	-37.102	5.003
24	6.824	-5.791	-56.719	7.078
25	6.699	-6.339	-49.364	6.300
26	6.301	-7.226	-54.866	6.882
27	7.097	-7.306	-56.747	7.081
28	6.824	-7.290	-56.850	7.092
29	6.208	-6.802	-51.035	6.477
30	7.444	-7.792	-58.173	7.232

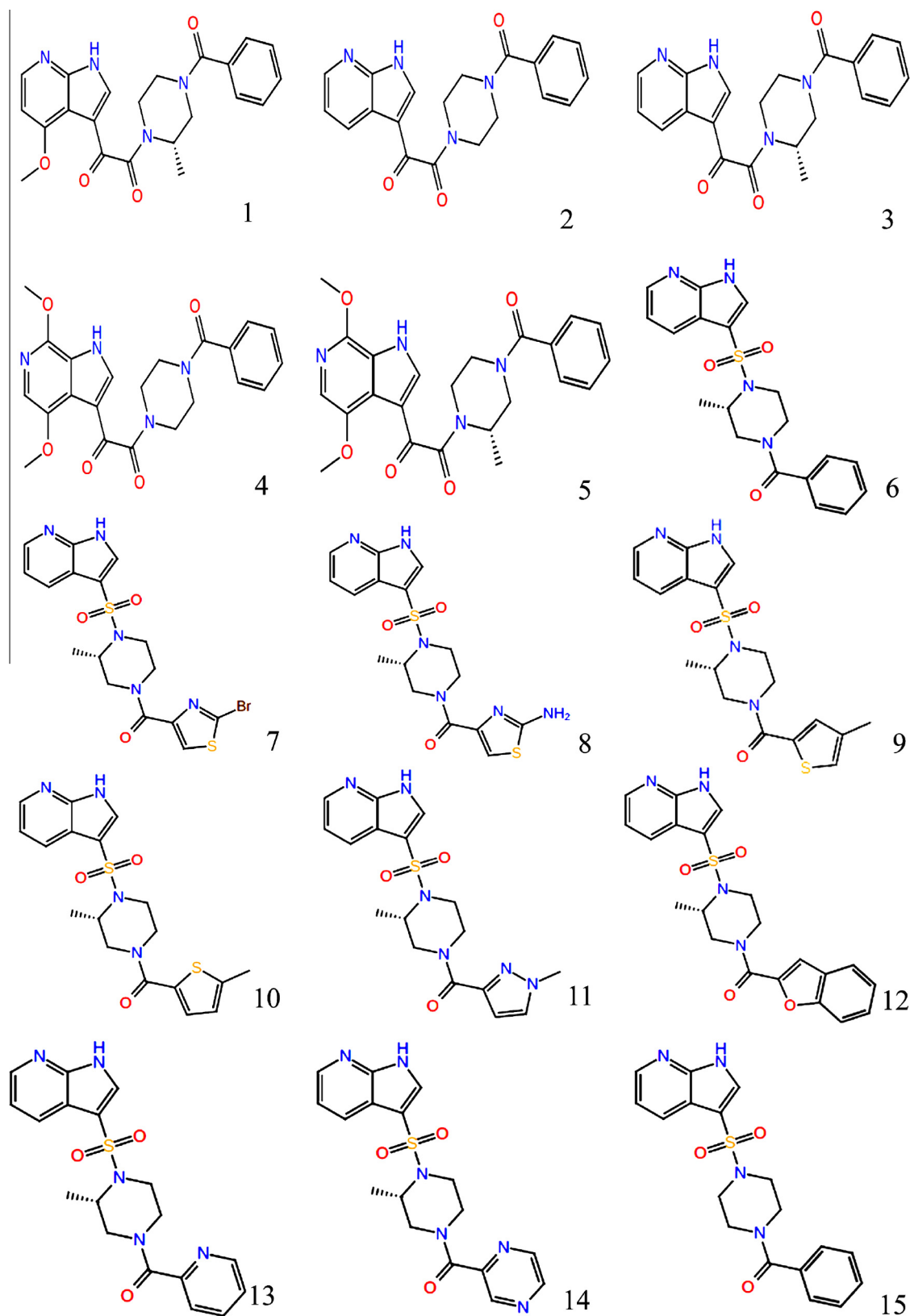


Figure 3. Structures of BMS derivatives.

resistance-conferring mutations.²¹ Phe43 cavity was chosen as target for computational simulations, a computational protocol based on molecular docking (induced fit docking), was applied to identify ligands targeting Phe43 cavity.

2.1. Molecular docking

Glide Score 5.6 XP^{22–25} is a harder function that exacts severe penalties for poses that violate established physical chemistry

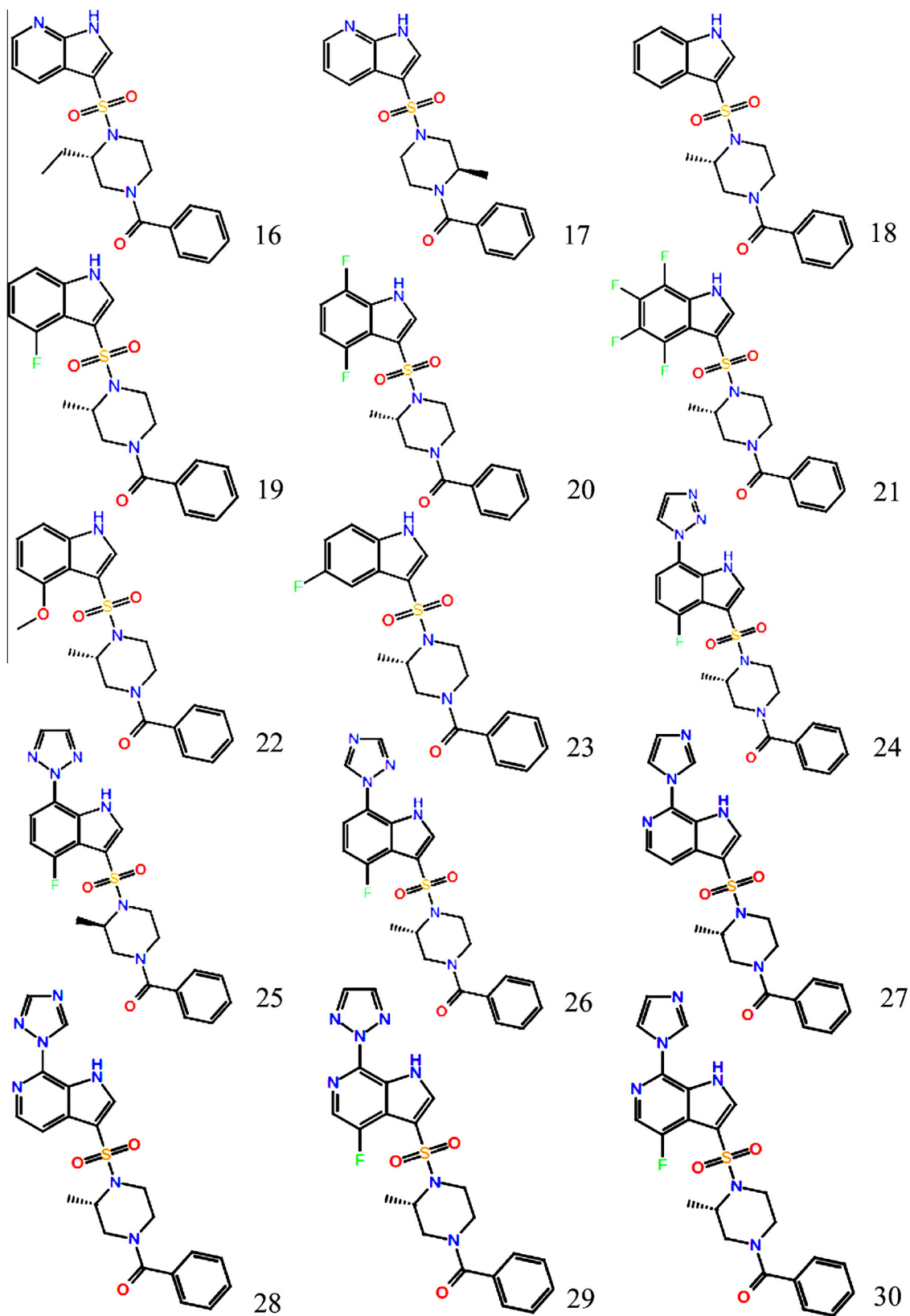


Fig. 3 (continued)

principles such as, charged and strongly polar groups should be adequately exposed to solvent. This minimizes false positives and is especially useful in lead optimization or other studies in which only a limited number of compounds will be considered experi-

mentally and each computationally identified compound needs to be as high in quality as possible. A combination of Glide Score, the ligand receptor molecular mechanics interaction energy, and the ligand strain energy is used to select the correctly docked pose.

This composite scoring function, is called as Emodel, it is much better at selecting the correct pose than, either the molecular mechanics energy or Glide Score alone. A regression analysis of biological activity (pIC_{50}) and Glide Emodel for known inhibitor was carried out. Correlation coefficient (r) of 0.768 and standard error of the estimate (s) of 0.62, model equation obtained from the regression is given below (Eq. 1), a scatter plot is shown in Figure 2. Glide Score, Emodel and predicted activity of the molecules are given in Table 1:

$$pIC_{50} = (-0.1058 \times \text{Emodel}) + 1.0773 \quad (1)$$

Analyses of protein–ligand interaction for the docked molecules display a similar binding mode as that of the Phe43 of CD4. In general, aromatic ring of benzoyl moiety linked to piperazine ring occupies the hydrophobic cavity of Phe43. Apart from these, molecules like 11, 12 and 13 (molecules shown in Fig. 3) having pyrazole, benzofuran and pyridine groups were observed to occupy the hydrophobic cavity. To have better understanding of protein–ligand interaction and to incorporate protein flexibility during docking run, an induced fit docking of BMS-806 (molecule 1), BMS-043 (molecule 4) and high potent derivative of BMS-806 (molecule 5) was carried out. Schrödinger's induced fit docking (IFD)^{26–28} protocol accounts for both small backbone relaxations in the receptor structure as well as significant side-chain conformational changes. This IFD protocol has been validated on a large set of pharmaceutically relevant examples with good results.^{27,28}

Dock pose of BMS derivatives into the Phe43 cavity showed a surprising match between the compound moieties and CD4 residues Ser42–Phe43–Leu44. Aromatic ring of benzoyl moiety linked to piperazine is seated deep into the CD4 Phe43 cavity than the phenyl ring of the CD4 Phe43. Binding pose of most potent derivative of BMS-806 (molecule 5) is shown in Figure 4, it clearly characterizes that the hydrophobic interaction at this cavity plays a major role in binding of inhibitors to gp120 receptor. A hydrogen bond interaction is seen between NH of the indole ring and residue Trp427. Based on these interactions it was summarized that molecules with hydrophobic groups that can be accommodated within the hydrophobic cavity and having some hydrogen bond donor groups that can interact with the hydrophilic region at the entry of the cavity comprising of residues Trp427, Asp368 would act as potential inhibitors.

To validate the assumption, a set of symmetrical N,N'-disubstituted ureas and thioureas (SU1–SU3) having benzimidazole and

Table 2

Glide Score, Emodel and predicted activity of symmetrical N,N'-disubstituted urea and thiourea

Compound	Glide Score (XP) (kcal/mol)	Emodel (kcal/mol)	Predicted activity
SU1	−7.458	−59.855	7.409
SU2	−6.027	−50.756	6.447
SU3	−6.667	−70.425	8.528
SU4	−8.992	−71.903	8.685
SU5	−6.356	−70.226	8.507
SU6	−7.260	−71.038	8.593
SU7	−8.868	−63.446	7.789
SU8	−8.163	−51.133	6.487
SU9	−8.157	−61.415	7.575
SU10	−8.130	−61.528	7.587
SU11	−7.411	−65.303	7.986
SU12	−8.698	−74.100	8.917

benzothiazole substitutions reported as antibacterial^{29,30} were docked by both the docking protocols (XP and Induced Fit). Their dock scores, Emodel and predicted activities are given in Table 2 and structures are shown in Figure 5. The dock poses obtained for these molecules were also similar to molecule 5, the benzimidazole ring was seating deep into the Phe43 cavity, and the NH of one of the benzimidazole had a hydrogen bond interaction with Asp368. Figure 6 represents the dock pose of SU1. SU3 having a 2-phenylbenzimidazole substitution, allows it to occupy an additional outer hydrophobic cavity, that increases its binding affinity, which is evident from its Emodel value of −70.425 kcal/mol. SU4 a thiourea compound having 2-phenylbenzimidazole, also showed a similar binding mode having a high Emodel value of −71.903 kcal/mol.

This encouraged us to design new symmetrical N,N'-disubstituted urea and thioureas having different fused heterocyclic group linked with urea or thiourea by methylene, phenyl and benzyl linker groups (SU4–SU12), preferably that can provide flexibility to the molecule to occupy hydrophobic cavity and also have hydrogen bond interaction with residues Trp427 and Asp368.

The Emodel, Glide Score, and predicted activity of these molecules are given in Table 2. Newly designed molecule SU12 showed the highest Emodel value, other molecules showed comparable values with that of existing inhibitors. Analysis of SU12 dock pose revealed that the heterocyclic group is occupying the hydrophobic

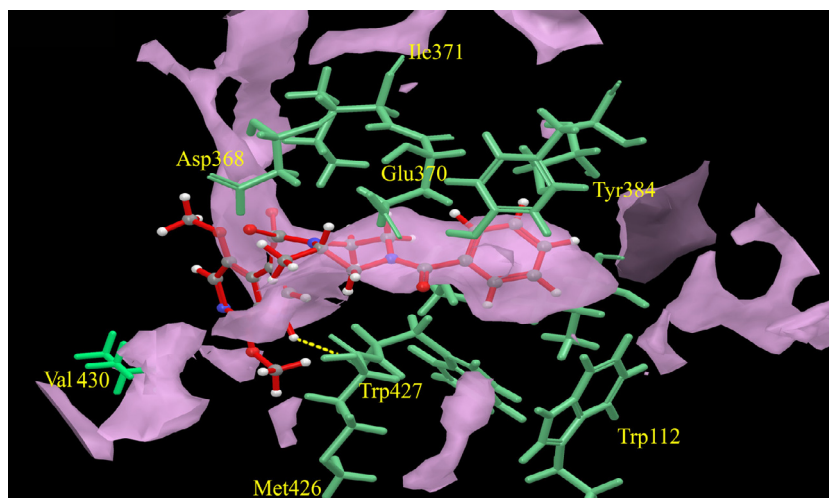


Figure 4. Dock pose of molecule five in the active site of HIV-1 gp120. The benzoyl group is occupying the hydrophobic cavity. The molecule shows a hydrogen bond interaction with residue Trp427 of HIV-1 gp120.

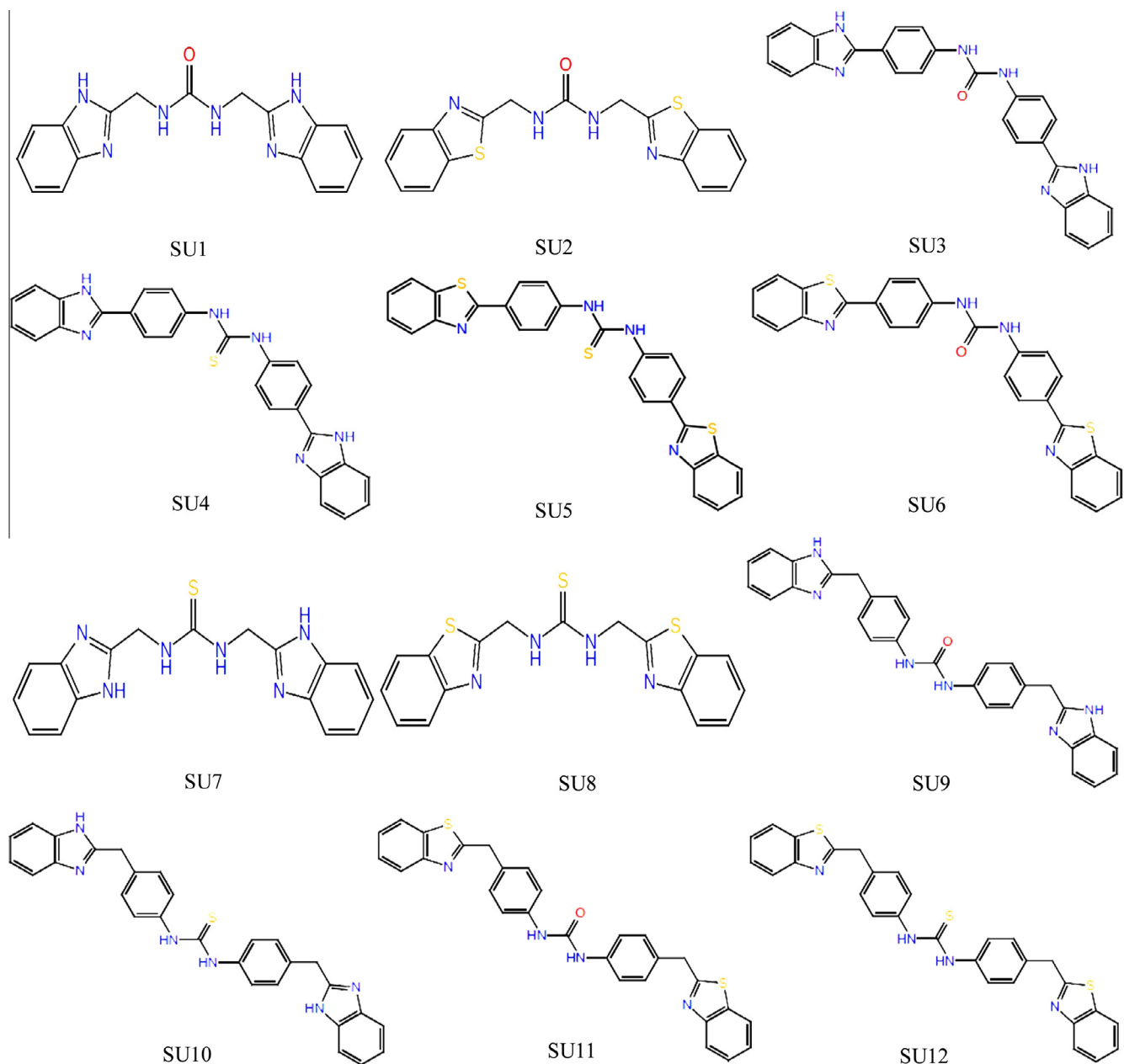


Figure 5. Structures of symmetrical N,N'-disubstituted urea and thiourea derivatives.

cavity inside the gp120 binding site of CD4, as well as it is having a favorable hydrophobic interaction with the residues at the entry site of the cavity. The molecule also has hydrogen bond interaction with residue Asp368 of HIV-1 gp120, which allows it to bind strongly to the receptor that is evident from its Emodel and GlideScore values of -74.10 and -8.969 kcal/mol, respectively. These symmetrical N,N'-disubstituted urea and thiourea molecules were synthesized using a novel microwave assisted synthetic procedure reported by us elsewhere and screened for their HIV-1 gp120 CD4 binding inhibitory activity.

2.2. Chemistry

The method applied for synthesis of symmetrical substituted urea/thiourea is summarized in Scheme 1. Amine hydrochlorides were reacted with urea or thiourea in 1:2 ratio using water medium under microwave irradiation for 4 min. Amine hydrochlorides

were prepared by the literature procedure,³¹ where *ortho*-phenylenediamine was condensed with aminocarboxylic acid in 5.5 M hydrochloric acid, refluxing for 12 h–3 days. Amine hydrochloride thus obtained was dried and reacted with urea or thiourea to yield symmetrical substituted urea/thiourea, and their final yields are provided in Table 3.

2.3. HIV-1 gp120–CD4 binding inhibition

Synthesized N,N'-symmetrical disubstituted urea and thioureas were screened for their HIV-1 gp120–CD4 binding inhibitory ability by HIV-1 gp120–CD4 capture Enzyme-linked immunosorbent assay (ELISA). All the screened compounds were found to inhibit HIV-1 gp120–CD4 binding in micromolar (0.013–0.247 μM) concentrations.³² Inhibitory activity (IC_{50}) values are listed in Table 4.

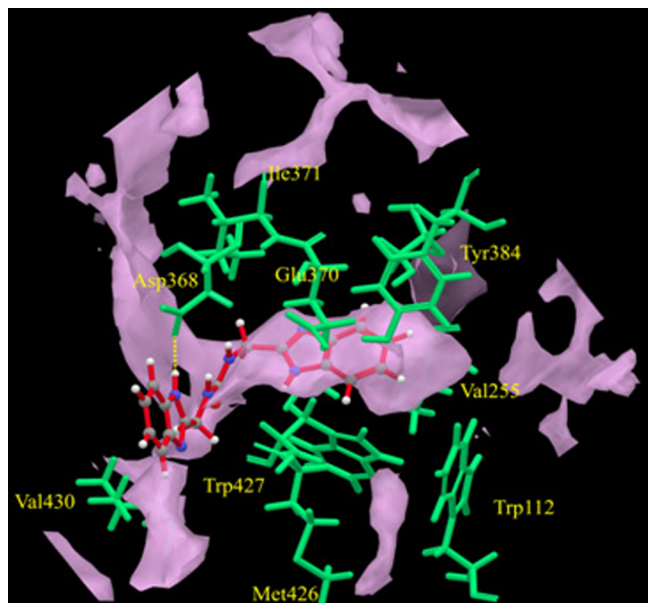


Figure 6. Dock pose of SU1 in the active site of HIV-1 gp120, the molecule is occupying the hydrophobic cavity in a similar manner as BMS derivative. It shows a hydrogen bonding interaction with residue Asp368 of HIV-1 gp120.

3. Conclusion

Highly improvised docking protocol was employed that can incorporate the protein flexibility during docking calculation. The dock pose analysis of the existing inhibitors of HIV-1 gp120 revealed important binding requirements, these include the need of a hydrophobic group that can interact with the hydrophobic cavity of CD4 Phe43 and also have hydrogen bond donor group that can interact with residues Trp427 and Asp368. These assumptions were validated by docking of symmetrically substituted urea and resulted in design of novel symmetrically substituted urea and thiourea derivatives that have potentials to act as CD4 mimic and inhibit the binding of HIV-1 gp120–CD4. These molecules were synthesized in aqueous medium using microwave irradiation. Study of inhibitory activity of these synthesized molecules has been carried out to prove its experimental validity and to further optimize the inhibitors.

4. Experimental

4.1. Docking studies

X-ray crystal structure of HIV-1 gp120 envelope glycoprotein complexed with CD4 and induced neutralizing antibody 17b with 2.2 Å resolution was downloaded from RCSB Protein Data Bank (<http://www.rcsb.org/pdb/home/home.do>) (PDB id: 1RZJ).³³ GLIDE

5.6 was used for ligand preparation, protein preparation and induced fit docking. The neutralizing antibody and CD4 chains were deleted, except for the Ser42–Phe43–Leu44 chain that binds to the HIV-1 gp120 cavity. Protein was prepared using protein preparation module applying the default parameters; considering Ser42–Phe43–Leu44 as ligand moiety. A grid was generated around these residues of CD4 with receptor van der Waals scaling for non-polar atoms as 0.9. A set of 30 known HIV-1 gp120 inhibitors having varied range of inhibition concentrations (IC_{50}) were selected from the literature³⁴ these were built using Maestro build panel and prepared by LigPrep application in Schrödinger 2010 suite. Molecular docking of 30 molecules into the generated grid was performed by using the extra precision (XP) docking mode.

Induced fit docking (IFD) protocol was run from the graphical user interface accessible within Maestro 9.0. It was carried out on prepared HIV-1 gp120 receptor with BMS-806, BMS-043 and high potent derivative of BMS-806 as test ligands (molecules 1, 4 and 5, respectively). The overall procedure has four stages: Briefly, during Stage 1 initial softened-potential Glide docking is performed on a van der Waals scaled-down rigid-receptor, a scaling of 0.7/0.5 was set for receptor/ligand van der Waals radii, respectively. The top 20 poses for each test ligand was retained. In Stage 2, receptor sampling and refinement was performed on residues within 5.0 Å of each ligand for each of the 20 ligand–protein complexes, followed by Prime^{35,36} side-chain sampling and prediction. The side-chains, as well as the backbone and ligand, undergo subsequent energy minimizations.

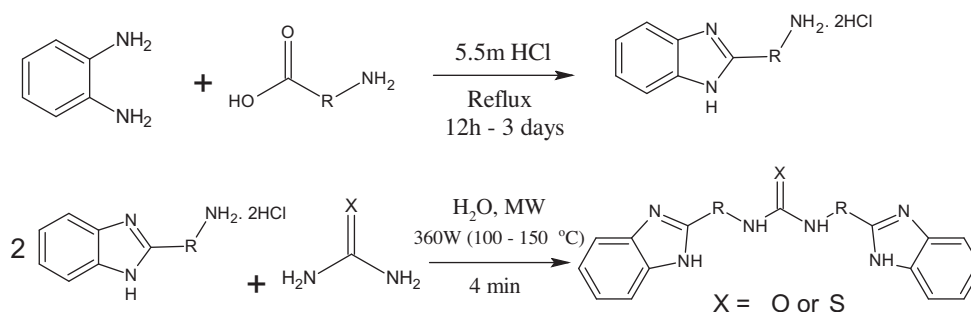
A total of 20 induced fit receptor conformations were generated for each of the test ligands. Stage 3 involved re-docking the test ligands into their respective 20 structures that are within 30.0 kcal/mol of their lowest energy structure. Finally, the ligand poses were scored in Stage 4 using a combination of Prime and Glide Score scoring functions in which the top ranked pose for each ligand was chosen as the final result. The XP scoring function was used in all docking stages.

4.2. General procedure for the preparation of heterocyclic amine hydrochlorides

To a mixture of *o*-phenylenediamine (0.01 mol) and aminocarboxylic acid (0.015 mol), 20 ml of 5.5 M hydrochloric acid was added and the reaction mixture was refluxed for 12 h–3 days at 150 °C. The reaction mixture was cooled for 12–18 h in a refrigerator to obtain the crystals of corresponding amine hydrochloride which were filtered, washed with ethanol and recrystallized from methanol.

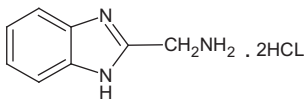
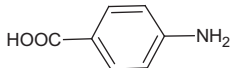
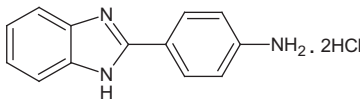
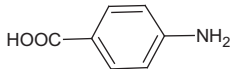
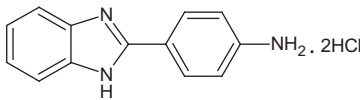
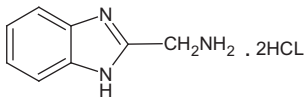
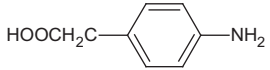
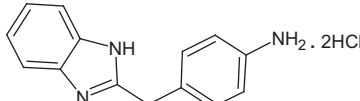
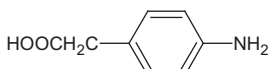
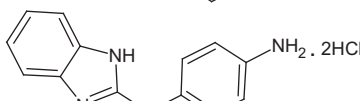
4.3. General procedure for the synthesis of symmetrical substituted urea

Amine hydrochlorides (0.02 mol) were thoroughly grinded with urea or thiourea (0.01 mol) in a borosil vessel, a paste of reaction



Scheme 1.

Table 3
Aminocarboxylic acids, amine hydrochlorides used for preparation of substituted urea/thiourea and obtained yields of disubstituted urea/thiourea

Compd	Aminocarboxylic acid	Amine hydrochloride	Yield ^a (%)
SU1	HOOCCH ₂ NH ₂	 . 2HCL	70
SU3		 . 2HCl	85
SU4		 . 2HCl	76
SU7	HOOCCH ₂ NH ₂	 . 2HCL	80
SU9		 . 2HCl	60
SU10		 . 2HCl	50

^a Yields refer to isolated and chromatographically pure products.

Table 4
HIV-1 gp120–CD4 binding inhibition (IC₅₀ values) for synthesized substituted urea and thiourea

S. No.	Compound	IC ₅₀ μM ± SD
1	SU1	0.247 ± 0.048
2	SU3	0.188 ± 0.036
3	SU4	0.126 ± 0.12
4	SU7	0.013 ± 0.1
5	SU9	0.197 ± 0.0032
6	SU10	0.149 ± 0.0073

mixture was made by adding few drops of water. Then the vessel was placed in synthetic microwave oven (Catalyst Cata 2R model) at 360 W power (100–150 °C) until the mixture was dry. Product was washed with water to remove any unreacted urea or amine hydrochloride. Solid was recrystallised from 1:1 methanol–water purified by column chromatography. Structures were confirmed by ¹H NMR, ¹³C NMR, IR, LC–MS and HRMS. ¹H NMR spectra were recorded in DMSO-*d*₆ on Bruker (Bio-spin) Ultrashield Arance-III Nano Bay 400 MHz NMR spectrometer and ¹³C NMR spectra were recorded in DMSO-*d*₆ on Avance 500 (125 MHz) spectrometer using SiMe₄ as internal standard. IR spectra were obtained on Tensor-27 (Bruker-optics) FTIR spectrophotometer using KBr disc. LC–MS were obtained on SHIMADZU 2010A. HRMS were obtained on Thermo Scientific LTQ Orbitrap.

4.3.1. *N,N*-Bis(1*H*-benzimidazol-2-ylmethyl)urea (SU1)

¹H NMR (DMSO-*d*₆, 400 MHz) δ 4.59–4.61 (d, 4H, *J* = 4.4 Hz), δ 7.25 (s, 2H), δ 7.33–7.34 (d, 4H), δ 7.64–7.65 (d, 4H). IR (KBr) band at 3361 and 1646 cm⁻¹ corresponding to NH and C=O stretching of amide group.

4.3.2. *N,N*-Bis[4-(1*H*-benzimidazol-2-yl)phenyl]urea (SU3)

¹H NMR (DMSO-*d*₆, 400 MHz) δ 6.60–6.61 (d, 4H, *J* = 2.4 Hz), δ 7.45–7.49 (q, 4H, *J*₁ = *J*₂ = 6 Hz), δ 7.69–7.72 (q, 4H, *J*₁ = *J*₂ = 6 Hz),

δ 7.74–7.77 (dd, 4H, *J*₁ = *J*₂ = 2.8 Hz), δ 10.62 (s, 2H). IR (KBr) band at 3298, 1629 cm⁻¹ corresponding to NH and C=O stretching of amide group. LC–MS: *m/z* (%) = 445 (M+1, 100).

4.3.3. *N,N*-Bis[4-(1*H*-benzimidazol-2-yl)phenyl]thiourea (SU4)

¹H NMR (DMSO-*d*₆, 400 MHz) δ 7.09–7.15 (complex peak), δ 12.50 (s, 2H); ¹³C NMR (DMSO-*d*₆, 125 MHz) δ = 109.42, 121.93, 132.07, 167.70 IR (KBr) band at 3153 and 1514 cm⁻¹ corresponding to NH and C=S stretching of thiocarbamide group. LC–MS: *m/z* (%) = 461 (M+1, 100).

4.3.4. *N,N*-Bis(1*H*-benzimidazol-2-ylmethyl)thiourea (SU7)

¹H NMR (DMSO-*d*₆, 400 MHz) δ 5.51–5.52 (d, 4H, *J* = 4.8 Hz), δ 8.27–8.30 (t, 2H, *J*₁ = 6 Hz, *J*₂ = 5.2 Hz), δ 8.46–8.51 (m, 4H), δ 8.58–8.60 (d, 4H, *J* = 8.4 Hz). IR (KBr) band at 3319 cm⁻¹ corresponding to NH stretching and 1531 cm⁻¹ corresponding to C=S stretching. LC–MS: *m/z* (%) = 337 (M+1, 100), HRMS (ESI), *m/z* calcd for C₁₇H₁₆N₆S (M+55(Na-CH₃OH adduct)) 391.1622, found 391.1657.

4.3.5. *N,N*-Bis[4-(1*H*-benzimidazol-2-ylmethyl)phenyl]urea (SU9)

¹H NMR (DMSO-*d*₆, 400 MHz) δ 4.10 (s, 4H), δ 7.12–7.13 (d, 4H, *J* = 3.2 Hz), δ 7.22–7.24 (d, 4H, *J* = 8 Hz), δ 7.37–7.39 (d, 4H, *J* = 7.6 Hz), δ 7.46–7.47 (d, 4H, *J* = 3.2 Hz), δ 8.64 (s, 2H). ¹³C NMR (DMSO-*d*₆, 125 MHz) δ = 33.55, 117.66, 120.84, 128.52, 130, 137.66, 151.88, 153.18. IR (KBr) band at 3601 and 1646 cm⁻¹ corresponding to NH and C=O stretching of amide group. LC–MS: *m/z* (%) = 473 (M+1, 100), HRMS (ESI), *m/z* calcd for C₂₉H₂₄N₆O (MH+) 473.2092, found 473.2071.

4.3.6. *N,N*-Bis[4-(1*H*-benzimidazol-2-ylmethyl)phenyl]thiourea (SU10)

¹H NMR (DMSO-*d*₆, 400 MHz) δ 4.38 (s, 4H), δ 7.35–7.37 (d, 4H, *J* = 8 Hz), δ 7.38–7.41 (q, 4H, *J* = 4 Hz), δ 7.52–7.54 (d, 4H, *J* = 8 Hz), δ 7.66–7.69 (q, 4H, *J* = 4 Hz), δ 10.19 (s, 2H). ¹³C NMR (DMSO-*d*₆,

125 MHz) δ = 32.06, 113.58, 117.76, 123.52, 128.87, 133.58, 138.01, 152.7, 178.81. IR (KBr) band at 3196 and 1512 cm^{-1} corresponding to NH and C=S stretching of thiocarbamide group. LC-MS: m/z (%) = 489 (M+1, 100), HRMS (ESI), m/z calcd for $\text{C}_{29}\text{H}_{24}\text{N}_6\text{S}$ (MH⁺) 489.1864, found 489.1833.

4.4. HIV-1 gp120-CD4 capture enzyme-linked immunosorbent assay (ELISA)

Commercially available CD4 Capture ELISA Kit (Product #102) was purchased from ImmunoDX, LLC. Several dilutions of positive reference CD4 (1000 ng/ml) in diluent buffer were prepared in Eppendorf tubes and labeled accordingly: 1000 ng/ml to 0.5 ng/ml in twofold serial dilutions. Test samples of compound to be analyzed were prepared using diluent buffer in 0.1–1000 ng/ml range. 100 μl of positive CD4 reference^{14–16} (1000 ng/ml) was added into the wells of the 96-well plates, to this test samples of different dilution were added, few wells were left blank for standard reference with different concentrations of positive reference CD4. The plate was incubated at room temperature for 1 h. Contents of the wells were discarded and the wells were washed three times with wash buffer. To this 100 μl of Anti-CD4 Peroxidase/detector reagent, 1:100 in diluent buffer was added, and incubated at room temperature for 1 h. Plate was washed five times with 1 \times wash buffer (300 μl /well), contents of wells were discarded and 100 μl of TMB substrate was added to each well, a blue color was allowed to develop for a period of 10 min at room temperature, the development of color was stopped by adding 50 μl of stop solution to each well, which resulted in change of color from blue to yellow. The absorption of contents of each well was read at 450 nm on SpectraMax M3 Multi-Mode Micro plate Reader from molecular devices within 15 min. Percent inhibition was calculated by using the following formula:

$$\% \text{ inh} = \frac{[(\text{Abs}^{450} \text{ CD4 reference (blank)}) - (\text{Abs}^{450} \text{ CD4 reference + test sample})]}{(\text{Abs}^{450} \text{ CD4 reference (blank)})} \times 100$$

4 Parameter Logistic or 4PL nonlinear regression model was applied for calculating IC_{50} values using MasterPlex 2010 software.

Acknowledgments

We gratefully acknowledge support for this research from DST (SR/FT/CS-040/2009), CSIR (01/(2436)/10/EMR-II) and UGC, New Delhi, India. We are thankful to Department of chemistry, Nizam College, Hyderabad, India where the research was carried out. We are grateful to Dr. M. Rupalatha, Duke University Medical Centre, North Carolina, for her timely help for carrying out HIV-1 gp120-CD4 binding assay for our compounds. We also acknowledge Schrödinger Inc. for GLIDE software, Tripos Inc. for SYBYLX-1.2. We are thankful to CFRD, Osmania University and IICT, Hyderabad for providing spectral data. We do not have any conflict of interest to declare.

Supplementary data

Supplementary data associated with this article can be found, in the online version, at <http://dx.doi.org/10.1016/j.bmc.2013.05.038>.

References and notes

1. Dalgleish, A. G.; Beverley, P. C.; Clapham, P. R.; Crawford, D. H.; Greaves, M. F.; Weiss, R. A. *Nature* **1984**, *312*, 763.

2. Borkow, G.; Lapidot, A. *Curr. Drug Targets: Infect. Disord.* **2005**, *5*, 3.
3. Harrison, S. C. *Adv. Virus Res.* **2005**, *64*, 231.
4. Kwong, P. D.; Doyle, M. L.; Casper, D. J.; Cicala, C.; Leavitt, S. A. *Nature* **2002**, *420*, 678.
5. Parren, P. W.; Moore, J. P.; Burton, D. R.; Sattentau, Q. J. *AIDS* **1999**, *13*, S137.
6. Wei, X.; Decker, J. M.; Wang, S.; Hui, H.; Kappes, J. C. *Nature* **2003**, *422*, 307.
7. Kwong, P. D.; Wyatt, R.; Robinson, J.; Sweet, R. W.; Sodroski, J.; Hendrickson, W. A. *Nature* **1998**, *393*, 648.
8. Vermeire, K.; Schols, D. *Expert Opin. Invest. Drugs* **2005**, *14*, 1199.
9. Kadow, J.; Wang, H. G. H.; Lin, P. F. *Curr. Opin. Invest. Drugs* **2006**, *7*, 721.
10. Lin, P. F.; Blair, W.; Wang, T.; Spicer, T.; Guo, Q.; Zhou, N.; Gong, Y. F.; Wang, H. G.; Rose, R.; Yamanaka, G.; Robinson, B.; Li, C. B.; Fridell, R.; Deminie, C.; Demers, G.; Yang, Z.; Zadjura, L.; Meanwell, N.; Colonna, R. *Proc. Natl. Acad. Sci. U.S.A.* **2003**, *100*, 11013.
11. Si, Z.; Madani, N.; Cox, J. M.; Chruma, J. J.; Klein, J. C.; Schön, A.; Phan, N.; Wang, L.; Biorn, A. C.; Cocklin, S.; Chaiken, I.; Freire, E.; Smith, A. B., III; Sodroski, J. G. *Proc. Natl. Acad. Sci. U.S.A.* **2004**, *101*, 5036.
12. Ho, H. T.; Fan, L.; Nowicka-Sans, B.; McAuliffe, B.; Li, C. B.; Yamanaka, G.; Zhou, N.; Fang, H.; Dicker, I.; Dalterio, R.; Gong, Y. F.; Wang, T.; Yin, Z.; Ueda, Y.; Matiske, J.; Kadow, J.; Clapham, P.; Robinson, J.; Colonna, R.; Lin, P. F. *J. Virol.* **2006**, *80*, 4017.
13. Zhao, Q.; Ma, L.; Jiang, S.; Lu, H.; Liu, S.; He, Y.; Strick, N.; Neamati, N.; Debnath, A. K. *Virology* **2005**, *339*, 213.
14. Yamada, Y.; Ochiai, C.; Yoshimura, K.; Tanaka, T.; Ohashi, N.; Narumi, T.; Nomura, W.; Harada, S.; Matsushita, S.; Tamamura, H. *Bioorg. Med. Chem. Lett.* **2010**, *20*, 354.
15. Narumi, T.; Ochiai, C.; Yoshimura, K.; Tanaka, T.; Ohashi, N.; Nomura, W.; Harada, S.; Arai, H.; Matsushita, S.; Tamamura, H. *Bioorg. Med. Chem. Lett.* **2010**, *20*, 5853.
16. Narumi, T.; Yoshimura, K.; Tanaka, T.; Ohashi, N.; Nomura, W.; Harada, S.; Arai, H.; Matsushita, S.; Tamamura, H. *Bioorg. Med. Chem.* **2011**, *19*, 6735.
17. Shimokawa, J.; Ishiwata, T.; Shirai, K.; Koshino, H.; Tanatani, A.; Nakata, T.; Hashimoto, Y.; Nagasawa, K. *Chem. Eur. J.* **2005**, *11*, 6878.
18. Carole, A. B.; Ray, S.; Cohen, F.; Shawn, K. C.; Larry, E. O. *J. Nat. Prod.* **2004**, *67*, 1319.
19. Kwong, P. D.; Wyatt, R.; Majeed, S.; Robinson, J.; Sweet, R. W.; Sodroski, J.; Hendrickson, W. A. *Structure* **2000**, *8*, 1329.
20. Wyatt, R.; Kwong, P. D.; Desjardins, E.; Sweet, R. W.; Robinson, J.; Hendrickson, W. A.; Sodroski, J. G. *Nature* **1998**, *393*, 705.
21. Xie, H.; Ng, D.; Savinov, S. N.; Dey, B.; Kwong, P. D.; Wyatt, R.; Smith, A. B., III; Hendrickson, W. A. *J. Med. Chem.* **2007**, *50*, 4898.
22. Glide version 5.6, Schrödinger, LLC., New York, 2010.
23. Friesner, R. A.; Banks, J. L.; Murphy, R. B.; Halgren, T. A.; Klicic, J. J.; Mainz, D. T.; Repasky, M. P.; Knoll, E. H.; Shelley, M.; Perry, J. K.; Shaw, D. E.; Francis, P.; Shenkin, P. S. *J. Med. Chem.* **2004**, *47*, 1739.
24. Halgren, T. A.; Murphy, R. B.; Friesner, R. A.; Beard, H. S.; Frye, L. L.; Pollard, W. T.; Banks, J. L. *J. Med. Chem.* **2004**, *47*, 1750.
25. Friesner, R. A.; Murphy, R. B.; Repasky, M. P.; Frye, L. L.; Greenwood, J. R.; Halgren, T. A.; Sanschagrin, P. C.; Mainz, D. T. *J. Med. Chem.* **2006**, *49*, 6177.
26. Schrödinger Suite 2010 Induced Fit Docking Protocol; Glide version 5.6, Schrödinger, LLC., New York, 2010.
27. Sherman, W.; Day, T.; Jacobson, M. P.; Friesner, R. A.; Farid, R. *J. Med. Chem.* **2006**, *49*, 534.
28. Farid, R.; Day, T.; Friesner, R. A.; Pearlstein, R. A. *Bioorg. Med. Chem.* **2006**, *14*, 3160.
29. Weitao, P.; Hua-Quan, M.; Xu, Y. J.; Elizabeth, C. N.; James, R. T.; Erik, C.; Armin, L.; Paul, K.; Alexander, S. K.; Wai, C. W.; Hu, L. *Bioorg. Med. Chem. Lett.* **2006**, *16*, 409.
30. Kitagawa, H.; Ozawa, T.; Iida, M.; Watanabe, T.; Takahata, S.; Yamada, M.; Yamamoto, Y. Japanese Patent 2006, WO 2007-JP51523 20070130.
31. Wu, H. Y.; Li, H.; Zhu, B. L.; Wang, S. R.; Zhang, S. M.; Wu, S. H.; Huang, W. P. *Transition Met. Chem.* **2008**, *33*, 9.
32. Manga, V., Sivan, S.; Madalla, R. Indian Patent Publication, Appl. No. 2522/CHE/2012, Publication date 5th October, 2012.
33. Huang, C. C.; Venturi, M.; Majeed, S.; Moore, M. J.; Phogat, S.; Zhang, M. Y.; Dimitrov, D. S.; Hendrickson, W. A.; Robinson, J.; Sodroski, J.; Wyatt, R.; Choe, H.; Farzan, M.; Kwong, P. D. *Proc. Natl. Acad. Sci. U.S.A.* **2004**, *101*, 2706.
34. Lu, R. J.; John, A. T.; Tatiana, Z.; Olga, K.; Vitalii, K.; Svetlana, K.; Sergey, S.; Jason, P.; Sagun, T.; Enugurthi, B.; Yang, Y.; Jian, W.; Stephanie, F.; Shelly, F.; Alana, S.; Jiyong, Z.; Sherry, S. O.; Michael, G.; Dani, B.; Brian, B.; Barney, K.; Peter, J.; Alisher, K.; Ma, Y. A.; Cynthia, J.; Changhui, L.; Tatiana, P.; Tong, Z.; Alexander, C.; Li, R.; Connie, S. *J. Med. Chem.* **2007**, *50*, 6535.
35. Prime version 2.2, Schrödinger, LLC., New York, 2010.
36. Jacobson, M. P.; Friesner, R. A.; Xiang, Z.; Honig, B. *J. Mol. Biol.* **2002**, *320*, 597.